

***Final Draft***  
**of the original manuscript:**

Stuenkel, S.; Drescher, A.; Wind, J.; Brinkmann, T.; Repke, J.-U.; Wozny, G.:  
**Carbon dioxide capture for the oxidative coupling of methane  
process – A case study in mini-plant scale**  
In: Chemical Engineering Research and Design (2011) Elsevier

DOI: 10.1016/j.cherd.2011.02.024

# Carbon Dioxide Capture for the Oxidative Coupling of Methane Process – A case study in mini-plant scale

S. Stünkel<sup>a</sup>, A. Drescher<sup>a</sup>, J. Wind<sup>b</sup>, T. Brinkmann<sup>b</sup>, J.-U. Repke<sup>a</sup>, and G. Wozny<sup>a</sup>

<sup>a</sup> Berlin Centre of Technology, Department of Process Engineering, Straße des 17. Juni 135, 10623

Berlin, Germany

<sup>b</sup> Helmholtz-Zentrum Geesthacht Centre for Materials and Coastal Research,  
Institute of Polymer Research, Max-Planck-Straße 1, 21502 Geesthacht, Germany

E-mail: Steffen.Stuenkel@tu-berlin.de

Phone: +49 30 314 79817

Fax: +49 30 314 26915

## Abstract

The Oxidative Coupling of Methane (OCM) to ethylene is a promising alternative for the oil based industry. In this process, beside the valuable product ethylene, unwanted by-products like CO<sub>2</sub> are produced. Hence, the gas stream has to be refined further. The process is not applied in the industry yet, because of high separation costs. This article focuses particular on the CO<sub>2</sub> purification of the OCM product stream. Therefore a case study was done for a design task of 90% CO<sub>2</sub> capture from 25 mol% in the OCM product gas with an operation pressure of 32\*10<sup>5</sup> Pa. Within the article is shown, how to resolve the lack of high separation cost for the purification and the development of an integrated, energy efficient CO<sub>2</sub> capture process for the OCM refinery is described. Therefore a state of the art chemical absorption process using Monoethanolamine (MEA) was developed and optimized for the base case. Therefore Aspen Plus<sup>®</sup> with the build-in rate based model for the mass transfer with an electrolyte NRTL – approach and chemical equilibrium reactions for the water-MEA-CO<sub>2</sub> system as well as kinetic reactions based on the MEA-REA package was applied. In order to improve the energetic process performance, gas permeation with dense membranes was studied as

process alternative. For this purpose a membrane unit was developed in Aspen Custom Modeler<sup>®</sup> (ACM). The solution-diffusion model with the free-volume-theory for gas permeation including Joule-Thomson effect as well as concentration polarization (Stuenkel, 2009) was applied successfully. Furthermore several selective layers for a composite membrane with experimentally determined parameters were studied by this model and it was found, that a matrimid membrane provides the best selectivity performance for the OCM CO<sub>2</sub> capture. Based on this material a membrane module was installed to form a hybrid separation process in combination with the amine based absorption process. The comparison of the state of the art process with the novel hybrid separation process shows an energy saving of more than 40% for the OCM CO<sub>2</sub> capture. In the experimental study the stand alone performance of each unit, as well as the performance of the hybrid process was studied and the results are presented in this article.

**Keyword:** Carbon Dioxide Capture, Membrane, Absorption, Oxidative Coupling of Methane, Hybrid Process

## **1. Introduction**

While the fossil fuel becomes shorter and the price for crude oil rises since the last decades provides the Oxidative Coupling of Methane a new route for the petrochemical industry, (Behr, 2010). The process based on a hot catalyzed gas phase reaction at temperatures up to 750 °C to converts methane to ethylene. Thus, the OCM opens up natural- or biogas as a new feedstock for a wide range of chemical products (Hall, 2005). Beside the desired product ethylene, unwanted by products like carbon dioxide are produced and the reaction product gas has to refine further. Due to high separation cost is this process not applied in industrial yet, although several process alternatives for the OCM are purposed in the literature (Salerno, 2010). So far, all purposed processes associated with high energy demand and cost-intensive downstream procedures for separation and gas recycling. To overcome the limitation, a novel approach of concurrent engineering is applied to study the whole process, including the down streaming simultaneously in a mini-plant scale (Deibele, 2006). In order to

investigate the whole OCM process from reaction over purification to separation in continuous operation, an integrated downstream concept was developed. Due to the yield limitation of 30 % for conventional OCM reactors, the goal of the downstream process synthesis is a further energetic and economic improved process performance to overcome the lack.

Figure 1

Hence, the whole process was divided into three units, shown in figure 1: the reaction unit, the purification unit and the separation unit; and all of them are investigated concurrently in a mini-plant scale. Furthermore, design cases were defined for the process synthesis of each unit under consideration of their interactions. Based on the general framework of figure 1, process conditions and the design task for the CO<sub>2</sub> separation unit was developed, which are given in table 1. The removal of acid gas components is a key step in the gas refinery to reach the product purity. Hence, for the CO<sub>2</sub> removal are several process options available, but for a selective removal is the chemical absorption process a state of the art process (Kohl, 1997; IPCC, 2005). Novel approaches like membrane separation reaches more interests and studied and discussed as well in this article.

Table 1

## **2. Base Case Design: Chemical Absorption Process**

A chemical absorption process using Monoethanolamine as a solvent was chosen to design a base case, which is presented in figure 2. Such a chemical absorption process is favored for species, which contains acid-based functional groups, like carbon dioxide. Another aspect is the fast kinetic of the MEA-CO<sub>2</sub> reaction, which affects the height of the absorption column, in order to provide a sufficient gas-liquid contact time. Those amine processes are well established and commonly used for industrial CO<sub>2</sub> separation. The advantages of amine processes are the high selectivity regarding CO<sub>2</sub>, reusing the solvent and recovering the heat by recuperation. Otherwise, they also cause high thermal energy demand for solvent regeneration in the desorption unit, that leads to several process concepts with improved energy performance. The concentration range of MEA in industrial plants is between 15 – 35 wt% (Kohl, 1997) and it was assessed for the base case by 30 wt%. Operating the column in an industrial relevant regime the F-Factor has to be in the range of 0.15 – 1.5 Pa<sup>0.5</sup>. The process was designed as simple as possible to handle a wide range of operation conditions and to build a proper base to compare process alternatives.

Figure 2

### *2.1 Simulation model*

The base case process was investigated theoretically and a simulation model was implemented by the commercial tool Aspen Plus<sup>®</sup>. Hence a rigorous process model was implemented using the provided build-in packages. This model includes the build-in electrolyte NRTL package ELECNRTL, with chemical equilibrium reactions for the liquid phase (Austgen, 1989) and the Redlich-Kwong equation of state for the gas phase. Furthermore the MEA-REA package was applied successfully in the packed column that considers the liquid phase reaction kinetics of the MEA with the CO<sub>2</sub>. The kinetic reactions are essential for the description of the rigorous model for the absorption (Kucka, 2003). The build-in RateSep approach was used to describe the mass transfer in the packed column. The discretization height per simulation segment of the absorption and desorption column was found with 0.1 m by a sensitivity study. Further increase shows no effect on the results of the CO<sub>2</sub> concentration profile, figure 1.

Figure 3

### *2.2 Parameter study and process design*

The effect of solvent flow rates on the regeneration energy demand was studied for the constant carbon capture of the design task iteratively. Hence, the reboiler heat duty was kept constant and the solvent flow rate was varied in a closed loop configuration (figure 2), to reach the design task of 90% CO<sub>2</sub> capture. Afterwards was the reboiler heat duty decreased in order to change the solvent regeneration and a new optimal solvent flow rate was found for the design case. The thermal regeneration energy demand was calculated per kg captured CO<sub>2</sub> from the raw gas. The aim of this procedure is to find the optimum between regeneration energy and solvent flow rate. The results for a particular gas load of 0.7 Pa<sup>0.5</sup> are presented in Figure 3 and table 2.

Figure 4

Table 2

Furthermore the effect of the column height on the captured CO<sub>2</sub> was studied in standalone simulation of the absorption column for each solvent flow. A minimal column height is necessary to realize the contact time of the liquid and the gas phase. Therefore the height of the column was increased for each flow rate till no effect on the CO<sub>2</sub> gas phase concentration (figure 2) was obtained. The column height was varied from 0.5 – 5 m and structured packing was chosen for the column internals. However, based on this simulation study was the process designed and developed for the

experimental study. While state of the art design procedures for process equipment are followed (Perry, 2008) and the key parameters of the process design are given in table 3.

Table 3

### *2.3 Experimental model validation*

To validate the simulation results and to study continuous operation, the process was build in a mini-plant scale, like the flow sheet and a photo shows (figure 2), while the technical details presented in table 3. A Sick-Maihak infrared online gas analyzer was used for Hydrocarbon and CO<sub>2</sub> detection with an accuracy of ±1%. Furthermore was a titration method developed for the liquid phase, to determine the CO<sub>2</sub> loading and the amine concentration with an accuracy of ±6%; ±10% respectively. In a first preliminary experimental study for different absorption pressure the desorption pressure effect on the regeneration was investigated and the simulation results was proofed experimentally. In table 4 are the experimental operation conditions presented for this preliminary study. In this study was the gas load, the raw gas feed pressure, the CO<sub>2</sub> raw gas concentration and the reboiler duty of the desorption column kept constant. While for different desorption pressure the flow rate was adapted, to reach the design task of 90% CO<sub>2</sub> capture. The simulation results are compared with the experimental data in figure 5. They are obtained for desorption top pressure of 2\*10<sup>5</sup> Pa with a solvent flow rate of 20 kg/hr.

Table 4

### *2.4 Results and discussion – preliminary experimental study*

The results of desorption top pressure variation are presented in table 5 for a standard absorption process configuration without any heat integration or process optimization. It was observed, that the minimum specific energy demand for this process conditions was achieved by 2\*10<sup>5</sup> Pa desorption top pressure. In this experimental study a solvent regeneration of 70 % was achieved. Thereby was the CO<sub>2</sub> loading of the rich solvent flow determined with 0.48 mol<sub>CO2</sub>/mol<sub>MEA</sub>; while the lean solvent flow was laded with 0.13 mol<sub>CO2</sub>/mol<sub>MEA</sub>. Furthermore shows the comparison of the experimental concentration profile for the absorption column a good agreement with the simulation results in figure 4, left side. While the prediction of the temperature profile by the simulation exhibit a large gap to the obtained experimental profile. Beside others, could the heat loss of none insulate absorption column a possible explanation for the discrepancy. Thus, the heat loss has to be taken in to account by the simulation model. Nevertheless seems the effect of temperature on the reaction kinetic or on the CO<sub>2</sub>

solubility negligible to reproduce the concentration profile by the simulation with a good agreement to the experiments, as figure 3 shows.

Table 5

#### *2.4 Base Case – experimental study results*

Consequently, the design case for an ordinary reactor gas stream was reproduced in the mini-plant, based on the results of the preliminary experimental study and they are presented in table 6. In this study could the design task of 90% CO<sub>2</sub> removal achieved by the operation conditions presented in table 7. The benchmark for a further process improvement was found with 5 MJ/kg<sub>CO<sub>2</sub></sub> with an ethylene loss of 6%. Remarkable on this result is the solvent regeneration of 15%, in comparison to 70 % found in the preliminary experimental study of chapter 2.4. Thus the solvent flow rate was increased by nearly 70% to achieve 90 % CO<sub>2</sub> removal in the base case compared to the flow rates of the preliminary experimental study.

Table 6

Table 7

### **3. Process alternatives**

#### *3.1 Process synthesis – alternative processes*

The design task of the purification unit is to deplete 90% of the carbon dioxide from reaction product stream. For a detailed process synthesis, particular substance property data are required and listed in Table 8.

Table 8

Several strategies are known for process synthesis (Kohl, 1997; Douglas 1995; Barnicki, 2004). The one, followed in this approach is a Knowledge-Based separation system synthesis (Barnicki, 1992). Following this procedure, the general separation tasks can be classified into: 1. Enrichment, 2. Sharp separation and 3. Purification. The enrichment is the concentration increase of a species in one of the product streams (Barnicki, 1992), whereas two high-purity product streams of two species resulting by sharp separation. While for the first separation class no high purity or high recovery is achievable, but with the second separation class two high purity or high recovery streams can be achieved. The classification of a sharp separation task can be proofed by the ration of the key components in the product streams, which has to be higher than 9 or less than 0.1 respectively. The key components for the CO<sub>2</sub> removal are the carbon dioxide (CO<sub>2</sub>), that has to remove and the ethylene (C<sub>2</sub>H<sub>4</sub>) as the

product. Purification, in this context represents the removal of one low concentration component, in this case study: the removal of CO<sub>2</sub> from 15 mol%. For the OCM design case, the sharp separation has to be considered to fulfil the task as a one step separation. However, it can be considered as a two step separation task as well, which consists of an enrichment followed by a purification separation. For all three separation tasks the applicable processes are presented in table 9, and discussed in detail in the next following sections.

Table 9

### 3.1.1. Cryogenic Distillation

Cryogenic distillation should apply only for high throughputs and is economical only for a volatility of the key components higher than two (Barnicki, 1992). For a system pressure of 32\*10<sup>5</sup> Pa results the relatively volatility to  $\alpha_{CO_2/C_2H_4} \approx 1$ , but for a system pressure of 1\*10<sup>5</sup> Pa becomes the relatively volatility to  $\alpha_{CO_2/C_2H_4} \approx 3$ , according to Figure 6. Thus, the cryogenic distillation at 32\*10<sup>5</sup> Pa should not applied, but, for a system pressure of 1\*10<sup>5</sup> Pa this process has to consider as an alternative. Hence, the cryogenic distillation was not considered as a process alternative for this design case of 32\*10<sup>5</sup> Pa.

Figure 6

### 3.1.2. Physical absorption

To consider the physical absorption as a applicable process for this separation task a selectivity for the key components of  $S_{CO_2/C_2H_4} > 4$  is recommended (Barnicki, 1992). The selectivity for two common physical absorbents: methanol and water was observed by using equation 2 in combination with the Henry approach, equation 2 and 3. Therefore the selectivity for methanol results to  $S_{CO_2/C_2H_4} = 1.11$  and for water as absorbent to  $S_{CO_2/C_2H_4} = 1.03$  respectively. The results show, that physical absorption should not considered as an alternative for the CO<sub>2</sub> removal of the OCM process.

$$S_{CO_2/C_2H_4}^{abs} = \frac{x_{CO_2}}{x_{C_2H_4}} \quad \text{Equation 1}$$

$$x_{CO_2} He_{CO_2} = y_{CO_2} P \quad \text{Equation 2}$$

$$x_{C_2H_4} He_{C_2H_4} = y_{C_2H_4} P \quad \text{Equation 3}$$



### *3.1.3. Chemical absorption*

Chemical absorption is favoured for species, which contains acid-based functional groups, like the carbon dioxide to remove them with high selectivity concerning valuable product. Several chemical absorbents are purposed in the literature like caustic potash, caustic soda or alkanolamines (Kohl, 1997). As state of the art absorbent in CO<sub>2</sub> separation alkanolamines are favoured with low molecular weight, low partial pressure, low corrosivity or no toxic behaviour (Thiele, 2007). Considering the physical and chemical properties of Alkanolamines, they are best suitable for CO<sub>2</sub> gas purification. Moreover exists several alkanolamines like Monoethanolamine (MEA), Diethanolamine (DEA) or Methyldiethanolamine (MDEA) and each of them with an particular field of application like low CO<sub>2</sub> partial pressure or sulphuric acid components (Kriebel, 2002). However, Monoethanolamine is the widespread used alkanolamine in CO<sub>2</sub> capture when a high selectivity is required. Therefore, Monoethanolamine with a concentration of 30 wt% was chosen for the chemical absorption process used in this article.

### *3.1.4. Molecular sieve and equilibrium adsorption*

To decide if molecular sieve adsorption is a proper alternative, the species have to differ in shape size and their kinetic diameters. The physical size properties of the commercial available adsorbents are listed in table 10. The components can be sized by their kinetic diameters based on table 8 as followed:  $\sigma_{C_2H_6} > \sigma_{C_2H_4} > \sigma_{CO_2} > \sigma_{CH_4} > \sigma_{N_2}$ . Remarkable is, that the kinetic diameter of the carbon dioxide is in the middle of the components and all diameters are very close together. Cause of this reason is the separation by size not efficient applicable and the molecular sieve adsorption was not considered as an alternative for the carbon dioxide removal. Equilibrium based adsorption is only suitable for species concentration less than 10 mol% and for a selectivity of the key components larger than 2. It was found, that the selectivity for equilibrium loading of the key components results to  $S_{CO_2/C_2H_4} = 1.74$ , based on experimental measurements for a 5A molecular sieve found in the literature (Pakseresht, 2002). Thus, the equilibrium adsorption was not taken into account as a process alternative.

Table 10

### *3.1.6. Condensation and catalytically conversion*

The separation by condensation should be considered when the difference in normal boiling point of the components is larger than 40 K. The separation by catalytic conversion is only suitable for

impurities. Cause of those reasons the condensation and catalytically conversion of the carbon dioxide was not took into consideration as proper process alternatives.

### *3.1.5. Membrane processes*

Considering membrane separation as an economical feasible separation technique, the selectivity of the key components should be larger than 15 (Barnicki, 1992). The selectivity for the key components can be obtained by the ratio of the permeability with equation 4.

$$\alpha_{CO_2/C_2H_4} = \frac{P_{CO_2}}{P_{C_2H_4}} = \frac{D_{CO_2} S_{CO_2}}{D_{C_2H_4} S_{C_2H_4}} \quad \text{Equation 4}$$

Permeability was determined by the pressure increase method for single gas components by the Hemholtz-Zentrum Geesthacht<sup>b</sup> (HZG). Based on their results the components selectivity was calculated for promising selective membrane materials and the results are presented in table 11. The most promising material for CO<sub>2</sub> removal from the OCM reaction product gas is a polyimide composite membrane, which consists of matrimide for the selective layer.

Table 11

### *3.1.7. Results for the alternative separation process synthesis*

The above discussion of recommended unit operation from table 9, shows that a membrane process can consider as an alternative process concept for the CO<sub>2</sub> separation from the OCM reaction product. The presence of hydrocarbons in the gas stream and the high feed pressure are the key factors that have to consider by the process synthesis for alternatives. Only tailor made separation processes can be applied to the OCM process for achieving high purity in combination with low product loss by low energy demand. Therefore either a one step separation process for a sharp separation can be applied or a two step separation process, consisting of enrichment and purification can be adopted. In the following section both cases are considered for the membrane process.

### *3.2. Membrane Processes as alternative CO<sub>2</sub> separation*

Gas permeation processes with dense membranes were applied as an efficient method to improve the energy demand of CO<sub>2</sub> capture (Baker, 2002). Therefore, they were investigated as an alternative in comparison to the base case. While industrial applications for gas permeation are rare, the potential of membrane in separation technique are vast and the applications rises (Brinkmann, 2006). Several materials like cellulose or polymer based materials can be used as a selective layer for the separation

of CO<sub>2</sub> from hydrocarbons (Lin, 2005). In this work were cellulose acetate (CA), polyethylene oxide (PEO), polydimethylsiloxane (PDMS) and matrimide (PI) investigated as selective layer with polydimethylsiloxane for the support layer in a HZG<sup>b</sup> composite flat sheet membrane configuration. Experiments for single gas permeation behavior were carried out by the HZG<sup>b</sup>, based on the pressure increase method.

### *3.2.1 Gas permeation membrane model*

First valuation of the separation efficiency was achieved by process simulation using the solution-diffusion model (Brinkmann,2006), equation 5 and was improved by applying the free-volume theory for temperature dependent gas permeation.

$$\dot{n}_i = \frac{S \cdot D}{\delta} \cdot \Delta f_{i,M} = \frac{P}{\delta} \cdot \Delta f_{i,M} \quad \text{Equation 5}$$

$$\dot{n}_i = L_i(T, c_i) \cdot \Delta f_{i,M} \quad \text{Equation 6}$$

For technical membranes the quotient of permeability  $P$  and membrane thickness  $\delta$  are combined to the permeance  $L$ , which has to be obtained experimentally. The permeance can be specified with the free-volume theory including temperature, pressure and concentration dependency. Furthermore are free-volume parameters obtained experimentally and parameters were adapted by the HZG<sup>b</sup>. The permeation flux describing equation using the permeance is given in equation 6 and forms the base of the developed model in Aspen Custom Modeler<sup>®</sup>. Beside the temperature and concentration dependency of the permeation behavior, the mass transfer and non ideal effects are taken into account. Those effects are the concentration polarization of the enriched component along the membrane and the Joule-Thomson effect of cooling by decompression of a real gas. Furthermore two different module structures were investigated in this model. The first structure treat the membrane as a one flat membrane with an overall length of 7.14 m and a wide of 0.07 mm, discretised with 100 steps over the whole length. While in the second structure the real module structure was taken into account as described below. The base of this structure is formed by one membrane sheet with the size parameter of table 12. The flow in a compartment is the flow between two baffles and was separated uniform to each membrane sheet of this compartment and the permeation behavior was

calculated only for one sheet. After the calculation of one sheet of the compartment, the flows were combined accordingly to the numbers of sheets in the compartment. In this way, the retentate of the compartment is the feed for the next compartment. The flow pattern is closer to the reality. The module structure is presented in table 12.

Table 12

### 3.1.2 One and two stage membrane process

Two different kinds of membrane processes were investigated in this study: a one stage membrane process and a two stage membrane process, presented in figure 7. The raw gas conditions for both processes were the same as for the base case and they are given in table 1 and 6. However, first screenings of the different materials were done, for a constant membrane area. Anticipate the results of the study, it was observed, that the design task of 90% CO<sub>2</sub> capture could be reached only with an ethylene losses of more than 40% by a one stage process. This is uneconomically for the OCM process. Hence a two step separation process was considered that consists of a membrane process followed by amine based absorption. The design tasks in particular are the reduction of the CO<sub>2</sub> concentration down to 15 vol% with the membrane and the rest has to remove by the following absorption process.

Figure 7

$$\text{Ethylene Loss} : \left( 1 - \frac{\dot{n}_{C_2H_4-Puregas}}{\dot{n}_{C_2H_4-Rawgas}} \right) \cdot 100\% \quad (4)$$

### 3.1.3 Experimental investigation

In the next step the simulation results were proofed by an experimental study with a HZG flat sheet envelope type membrane module of 0.5 m<sup>2</sup> composite membrane with matrimide as the selective layer. In order to understand the membrane behavior, preliminary experiments were carried out for the stand alone membrane module, with which the effect of feed pressure, CO<sub>2</sub> concentration and velocity was investigated. In table 8 are the varied parameter and their range presented. The structure of the module with their particular compartments and sheets are given in table 12.

Table 13

### 3.1.4 Results

The simulation results for the CO<sub>2</sub> and the C<sub>2</sub>H<sub>4</sub> concentration in the retentate side are compared with the experimental results and presented in figure 8. While the simulation results for the CO<sub>2</sub> concentration in the retentate side with the detailed module structure represents the experiments with an average error of 10%. In comparison to this, the model with the one sheet structure represents the experiments with 20% error for the CO<sub>2</sub> concentration in the retentate side. Whereas the simulation results for the detailed module structure for the C<sub>2</sub>H<sub>4</sub> concentration represents the experiments with an average error of 8.4 %. While, in comparison to this, the one sheet structured model represent the experiments with 6.8 % error for C<sub>2</sub>H<sub>4</sub> in the retentate side. Consequently is the agreement of simulation with experiments for the C<sub>2</sub>H<sub>4</sub> better than for the CO<sub>2</sub> concentration. Nevertheless is the prediction for experiments of more than 13 vol% CO<sub>2</sub> feed concentration with an average error of 2.4% much better than the prediction of experiments with lower CO<sub>2</sub> feed concentration with an error of 45%. Generally can be resumed that simulation model of the detailed membrane structure represents the real behavior well with a maximum error of 10% and the model can be used to optimize the process.

Figure 8

#### **4. Hybrid Process: combined Membrane-Amine Process**

To fulfill the design task, a membrane process was combined with an absorption process and results in a hybrid process (Figure 9). While the membrane unit removes 50% of the CO<sub>2</sub> down to 15 vol%, the absorption process removes the rest of the CO<sub>2</sub> down to 1 vol%. This process fulfills the design task of more than 90% CO<sub>2</sub> capture with an experimentally determined thermal energy demand of only 2.78 MJ/kg<sub>CO<sub>2</sub></sub>. Thus an energy saving of more than 40% was achieved by using the hybrid process in comparison with the base case. Whereas the hybrid process product losses is with 13.3 % acceptable, but higher than those of the base case. The detailed experimental results of the hybrid separation process are presented in table14, 15 and 16. The performance of the membrane unit in the hybrid separation unit is listed in table 14, those of the absorption unit are listed in table 15 and the overall performance of the hybrid process is listed in table 16.

Figure 9

Beside the energetic aspect, the process flexibility is an advantage of the hybrid process, to handle a wide range of CO<sub>2</sub> concentration by using the membrane and absorption process, separated or together. Nevertheless improves the hybrid process the overall economics, achieves 40% of energy

saving and reduces investment cost due to smaller equipment size for components like the column, reboiler, condenser and pumps. In contrast, only additional investment costs have to be spent for the membrane module of the hybrid process. However, the developed models were validated successfully and can be used for the process optimization.

Table 14

Table 15

Table 16

## **7. Conclusions**

Within this article was the design and development of an alternative separation process presented. This process was compared to a state of the art process in order to improve the energetic performance for constant carbon capture. As a side condition the product loss was chosen and was evaluated. Nevertheless a case study was presented for the CO<sub>2</sub> capture of the OCM Process. Therefore was a single membrane unit, a two stage membrane unit, a stand alone absorption process and the combination of a membrane with an absorption process to a hybrid separation process studied and discussed. As a result a hybrid separation process was developed, based on rigorous simulation that saves more than 40 % energy in comparison to the base case with acceptable product losses. Furthermore was the rigorous simulation model validated experimentally in the installed mini-plant and the hybrid separation process was reproduced experimentally.

## **Acknowledgements**

The authors acknowledge the support from the Cluster of Excellence "Unifying Concepts in Catalysis", coordinated by the Berlin Institute of Technology and funded by the German Research Foundation (DFG).

## Notation

$\alpha$	[-]	selectivity
$\sigma$	[Å]	Lenard Jones diameter
$\delta$	[m]	membrane thickness
$c$	[mol/m <sup>3</sup> ]	concentration
$D$	[m <sup>2</sup> /s]	Diffusion coefficient
$f$	[Pa]	Fugacity
$H_e$	[Pa]	Henry coefficient
$L$	[mol/Pa m <sup>2</sup> s]	Permeance
$\dot{n}$	[mol/s m <sup>2</sup> ]	molar flux
$p$	[Pa]	pressure
$P$	[mol/Pa m s]	Permeability
$S$	[mol/m <sup>3</sup> Pa]	Solubility coefficient
$T$	[K]	Temperature
$x$	[-]	liquid molar fraction
$y$	[-]	vapour molar fraction

## References

Austgen, D. M., Rochelle, G. T., Peng, X., Chen, C. C. ,1989. Model of vapor–liquidequilibria for aqueous acid gas–alkanolamine systems using the Electrolyte-NRTL equation. *Industrial & Engineering, Chemistry Research*, 28, 1060–1073.

Baker, Richard W., 2002. *Future Directions of Membrane Gas Separation Technology*, Ind. Eng.Chem. Res. 41, 1393 -1411

Barnicki, S. D.; Fair, J., R.; 1992. *Separation System Synthesis: A Knowledge-Based Approach: 2. Gas/Vapor Mixtures*, Ind. Eng. Chem. Res., 31, 1679-1694

*Carbon Dioxide Capture for the Oxidative Coupling of Methane Process – A case study in mini-plant scale*

Barnicki, S. D.; Sirola, J. J.; 2004. Process synthesis prospective, Computers and Chemical Engineering, 28, 441 - 446

Behr, A.; Kleyensteiber, A; Hartge U.. 2010, Alternative Synthesewege zum Ethylene, Chemie Ingenieur Technik, Volume 82, Issue 3, 201–213,

Bird, B. R.; Stewart, W. E., Lightfoot, E. N., 2007. Transport Phenomena, John Wiley & Sons,

Brinkmann, T., 2006. Modellierung und Simulation der Membranverfahren Gaspermeation, Dampfpermeation und Pervaporation in: Ohlrogge and Ebert (Eds.), 2006, Membranen, Wiley-VCH, pp. 273 - 333

Deibele, L.; Dohm, R.; 2006. Miniplant-Technik, WILEY-VCH Verlag GmbH & Co. KGaA, Weinheim

Douglas, J. M., 1995. Synthesis of separation system flowsheets, AIChE – Journal, Vol. 41, No. 12

Lin, H., Freeman, B. D., 2005. Materials selection guidelines for membranes that remove CO<sub>2</sub> from gas mixtures, Journal of Molecular Structure, 739, 57–74

Hochgesand, G., 2002. Gas treatment in Gas Production, Ullmann's Encyclopaedia of Industrial Chemistry, Wiley – VCH, Weinheim,

Hall, K. R., 2005. A new gas to liquids or gas to ethylene technology, Catalysis today, vol. 106, pp. 243

IPCC, 2005: IPCC Special Report on Carbon Dioxide Capture and Storage. Cambridge University Press, Cambridge, NY, USA, pp. 109 -111



*Carbon Dioxide Capture for the Oxidative Coupling of Methane Process – A case study in mini-plant scale*

Jaso, S.; Godini, H. R.; Arellano-Garcia, H.; Wozny, G., 2010. Oxidative Coupling of Methane: Reactor Performance and Operating Conditions, Computer Aided Chemical Engineering, Volume 28, Pages 781-786

Kohl A. L., Nielsen R., 1997. Gas Purification, 5th edition, Gulf Pub Co,

Kucka, L., Mueller, I., Kenig, E. Y., Gorak, A., 2003. On the modelling and simulation of sour gas absorption by aqueous amine solutions; Chemical Engineering Science, vol. 58; pp. 3571 – 3578

Kriebel, M., Schlichting H., 2002. Absorption in Gas Production, Ullmann's Encyclopedia of Industrial Chemistry, Wiley – VCH, Weinheim,

Pakseresht S., Kazemeini M., Akbarnejad M., 2002. Equilibrium Isotherms for CO, CO<sub>2</sub>, CH<sub>4</sub>, C<sub>2</sub>H<sub>4</sub> on the 5A molecular sieve by a simple volumetric apparatus, Separation and Purification Technology, Vol. 28, Iss. 1, pp. 53-60

Perry, R. H., Green, D. W., 2008. Perry's Chemical Engineers' Handbook, Section 14: Equipment for Distillation, Gas Absorption, Phase Dispersion, and Phase Separation, McGraw-Hill

Salerno, D., Arellano-Garcia, H., Wozny, G., 2010. An Alternative Process for Oxidative Methane Coupling for Ethylene, Electricity and Formaldehyde Production, presentation on AIChE Annual Meeting, 7.11.- 12.11., Salt Lake City, USA

Stünkel, S., Litzmann, O., Repke, J.-U. and Wozny, G., 2009. Modeling and simulation of a hybrid separation process for the carbon dioxide removal of the oxidative coupling of methane process, Computer Aided Chemical Engineering, Volume 26, p. 117-122

Thiele, R. 2007. Selective Absorption innerhalb der Kokereigasreinigung, Dissertaion TU-Berlin

Figures - colored

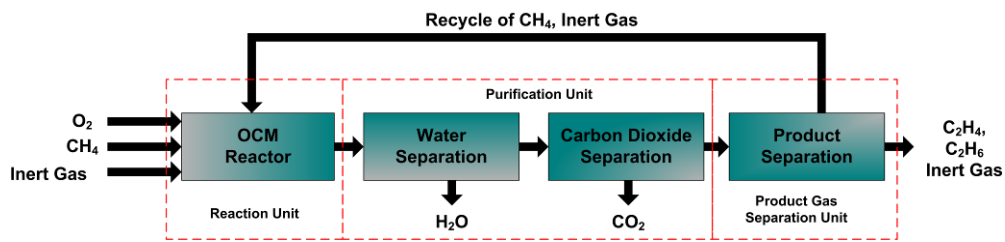


Figure 1. Flow diagram of the OCM – Process

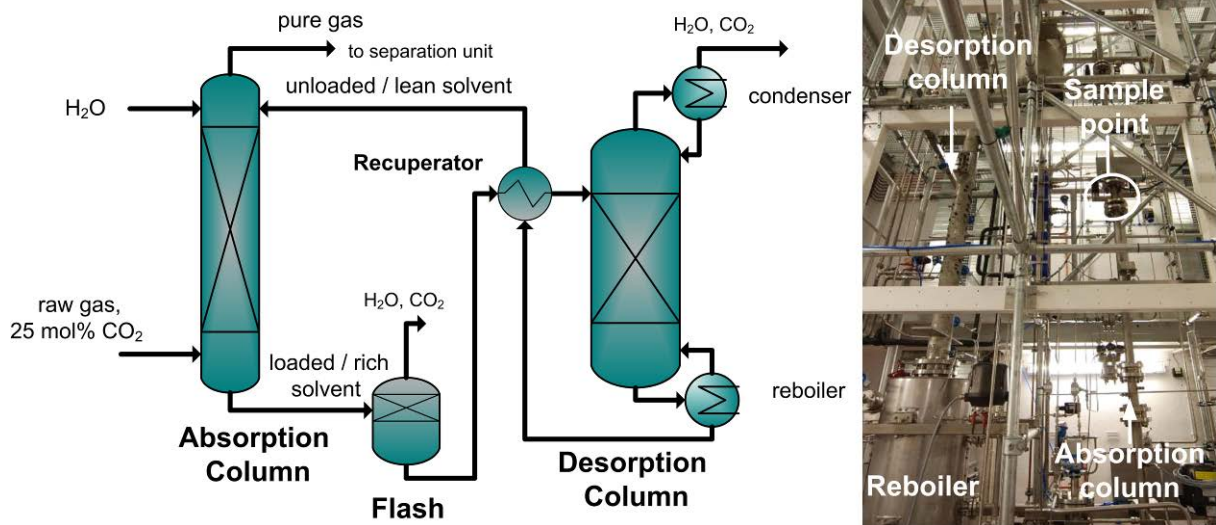


Figure 2. Flow sheet of the amine based absorption process and photo of the mini-plant process

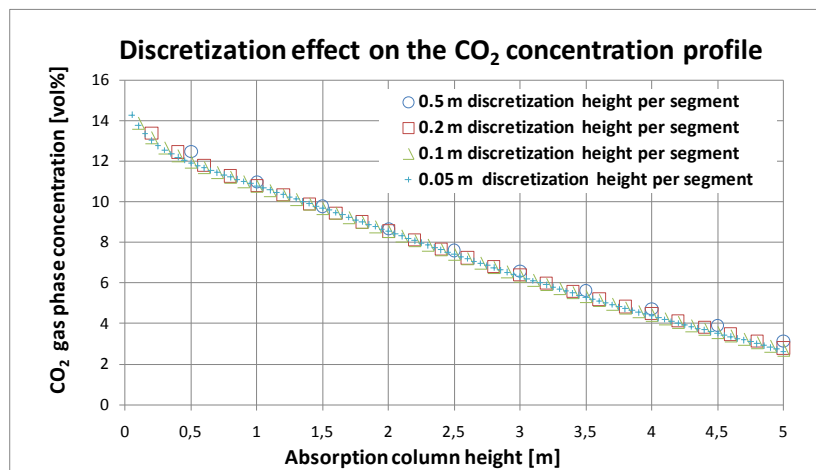


Figure 3. Effect of absorption column discretization on concentration profile

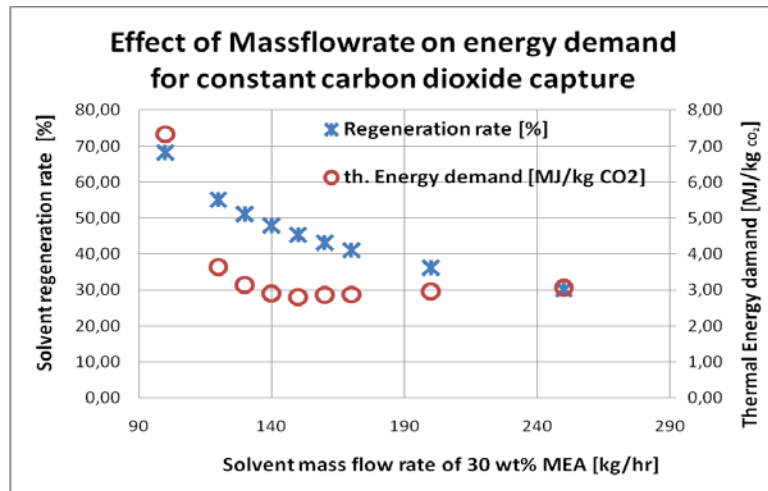


Figure 4. Simulation results – thermal energy demand for different solvent flows with constant carbon capture

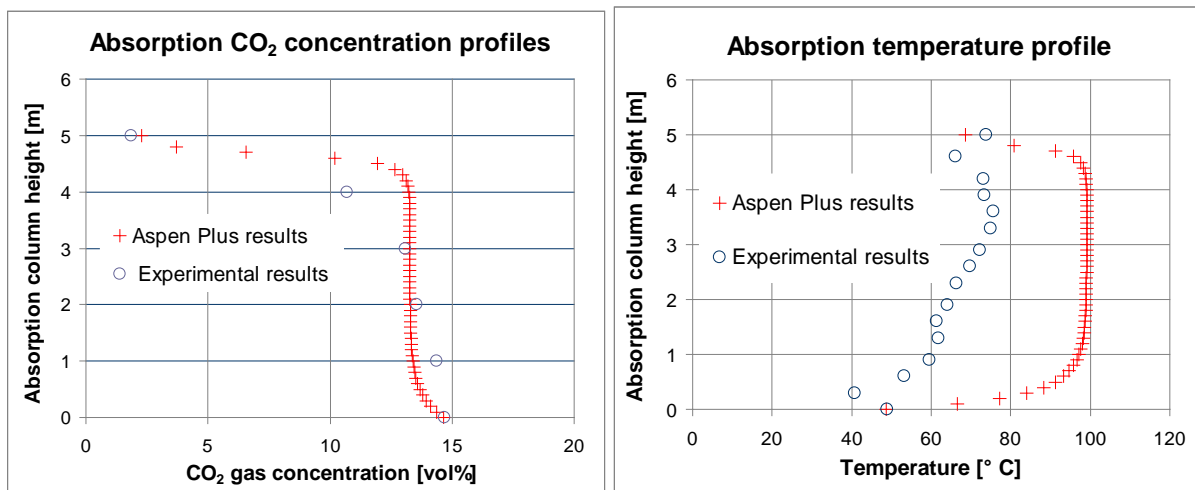


Figure 5. left side: Comparison simulation results for CO<sub>2</sub> concentration profile with the experiments, right side: comparison of experimental absorption temperature profile with simulation result

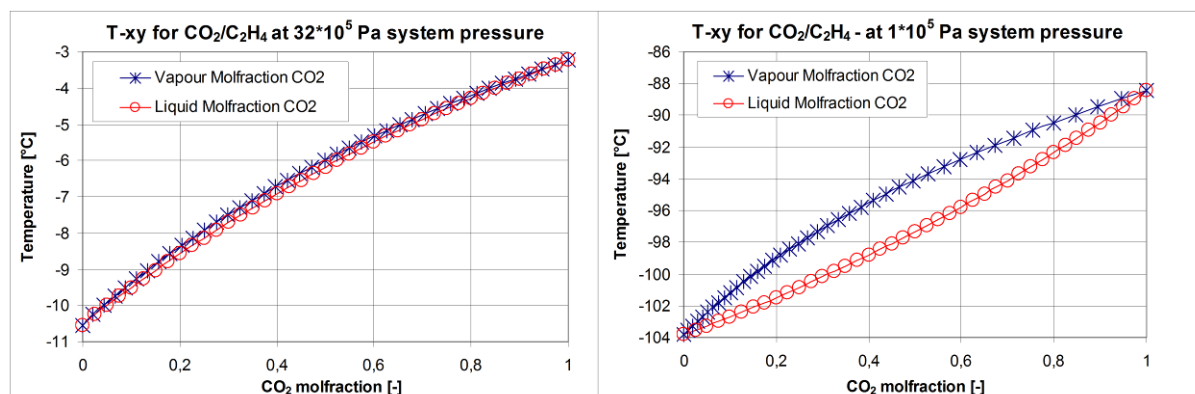


Figure 6. Vapor liquid equilibrium for CO<sub>2</sub>/C<sub>2</sub>H<sub>4</sub> to determine the relatively volatility at 32\*10<sup>5</sup> Pa left side and 1\*10<sup>5</sup> Pa, right side

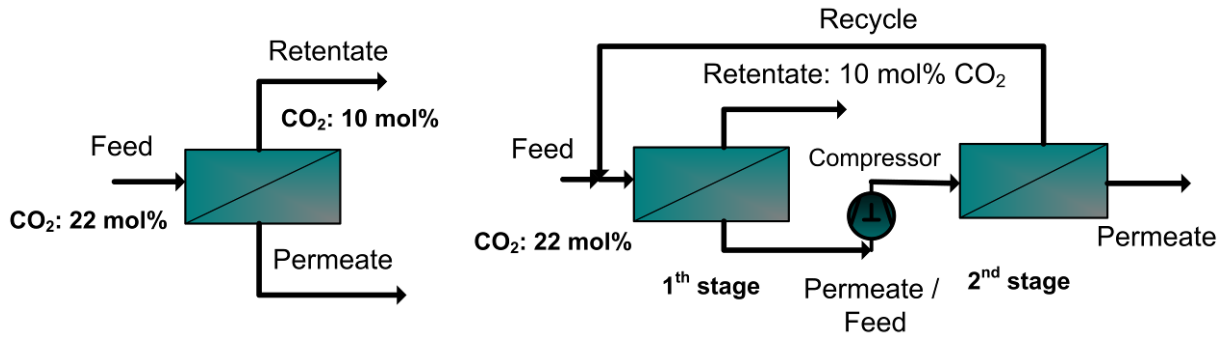


Figure 7. Left side: One stage membrane process – right sight: Two stage membrane process

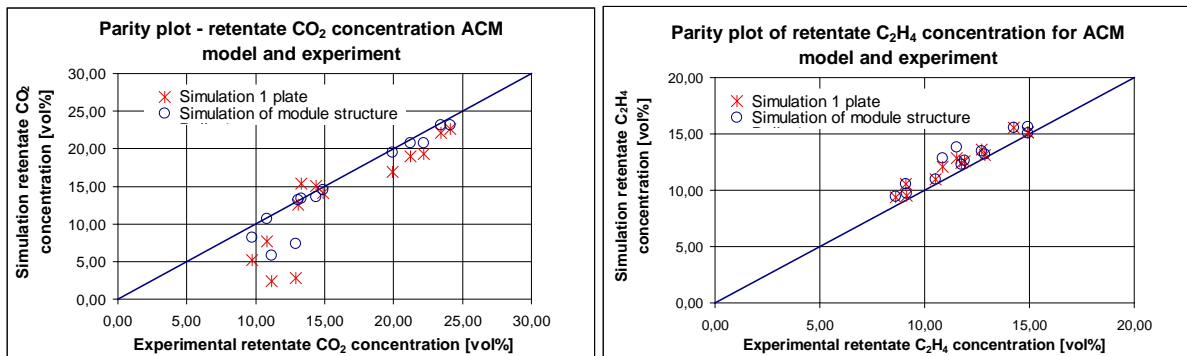


Figure 8. Parity plot between experimental and simulation retentate results for CO<sub>2</sub> concentration (left side) and C<sub>2</sub>H<sub>4</sub> concentration (right side)

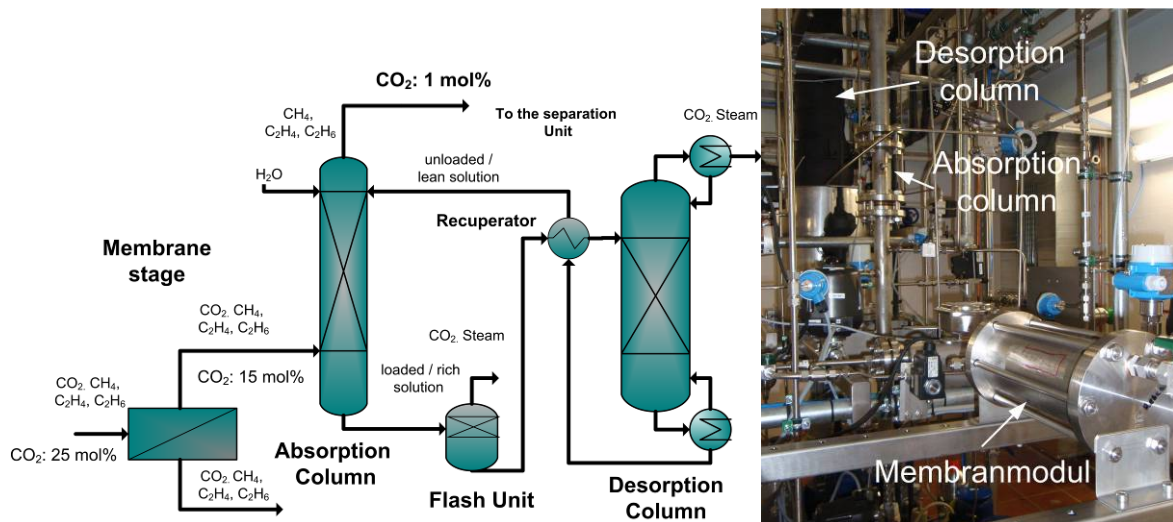


Figure 9. Left side: Flow diagram of the hybrid CO<sub>2</sub> capture process: combined membrane and absorption process; right side: mini-plant design for experimental investigations

Figures – gray scale

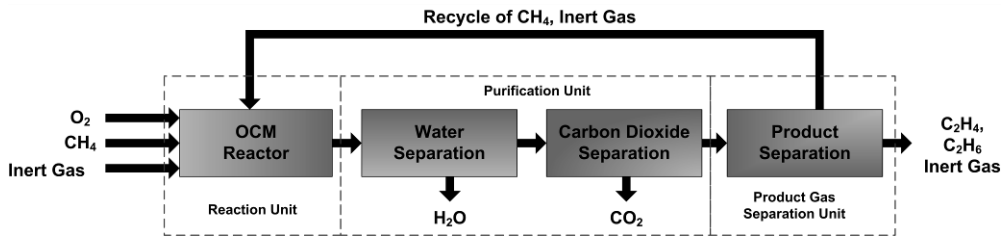


Figure 1. Flow diagram of the OCM – Process

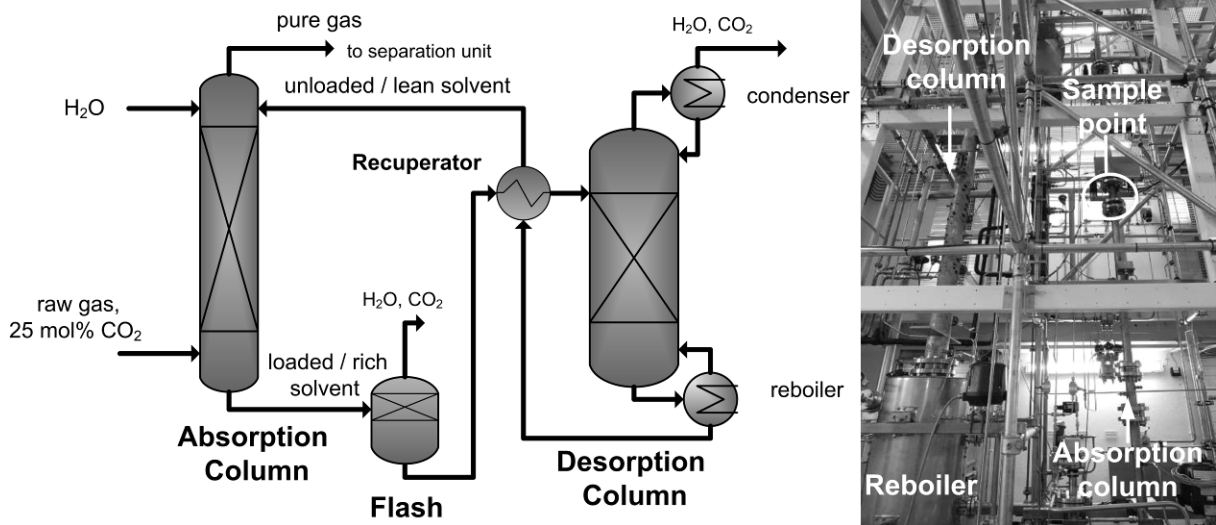


Figure 2. Flow sheet of the amine based absorption process and photo of the mini-plant process

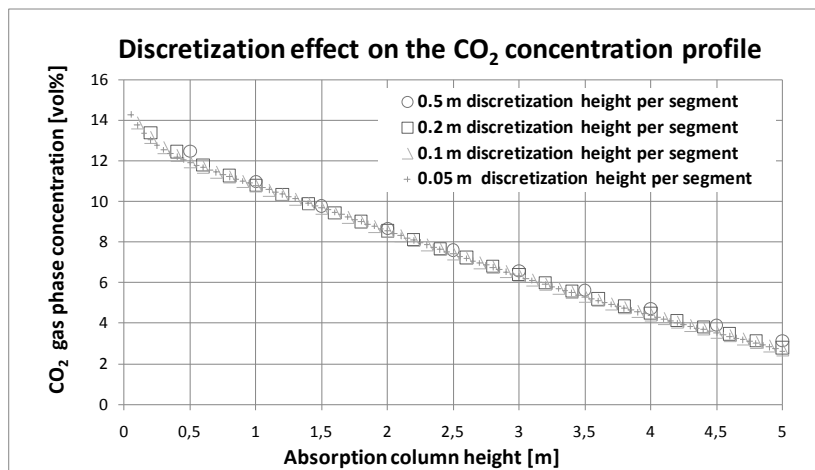


Figure 3: Effect of absorption column discretization on concentration profile

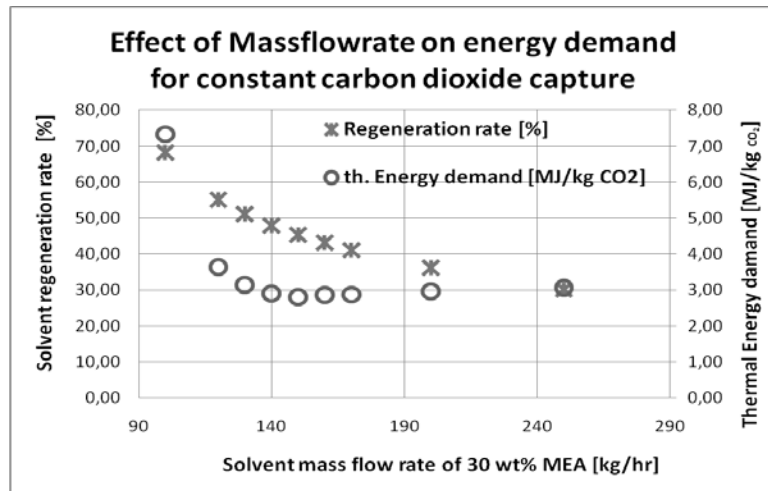


Figure 4. Simulation results – thermal energy demand for different solvent flows with constant carbon capture

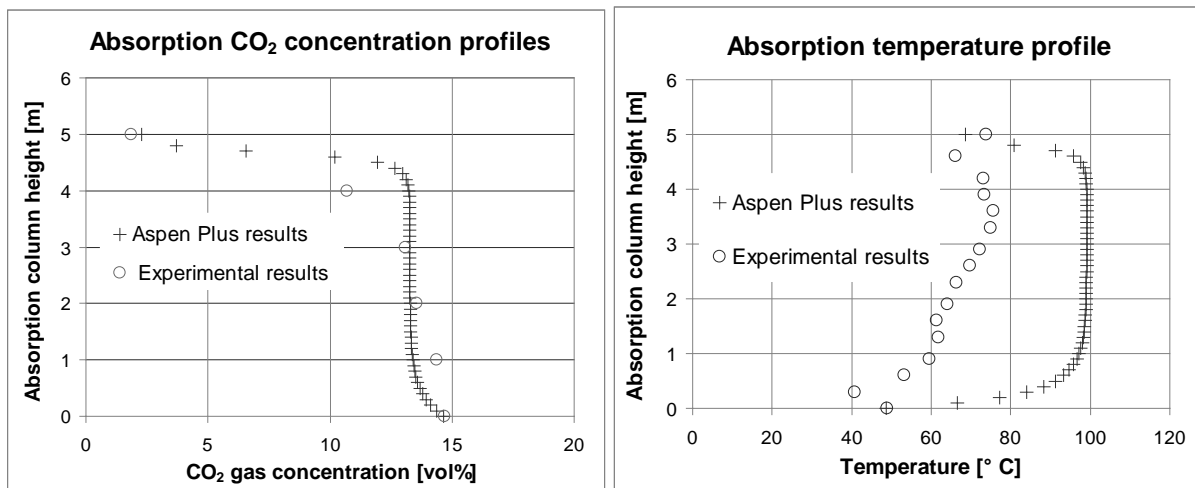


Figure 5. left side: Comparison simulation results for CO<sub>2</sub> concentration profile with the experiments, right side: comparison of experimental absorption temperature profile with simulation result

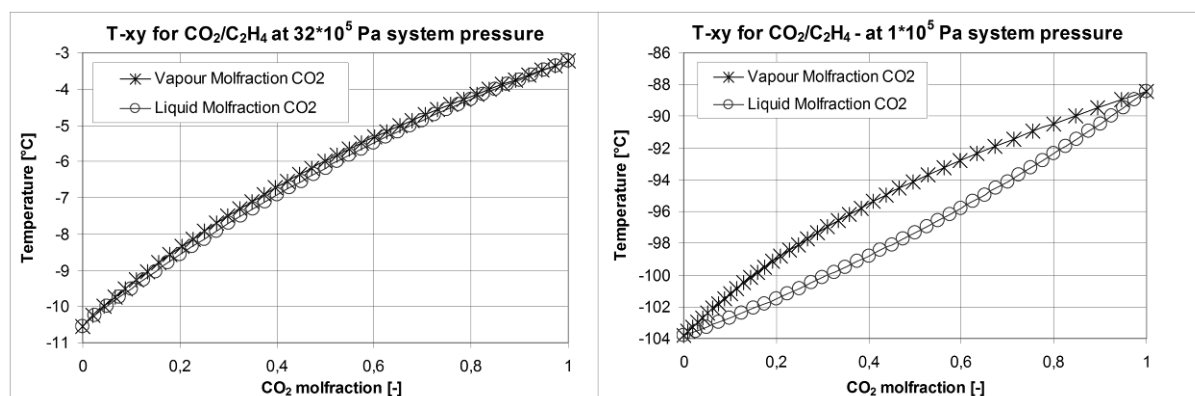


Figure 6: Vapor liquid equilibrium for CO<sub>2</sub>/C<sub>2</sub>H<sub>4</sub> to determine the relative volatility at 32\*10<sup>5</sup> Pa left side and 1\*10<sup>5</sup> Pa, right side

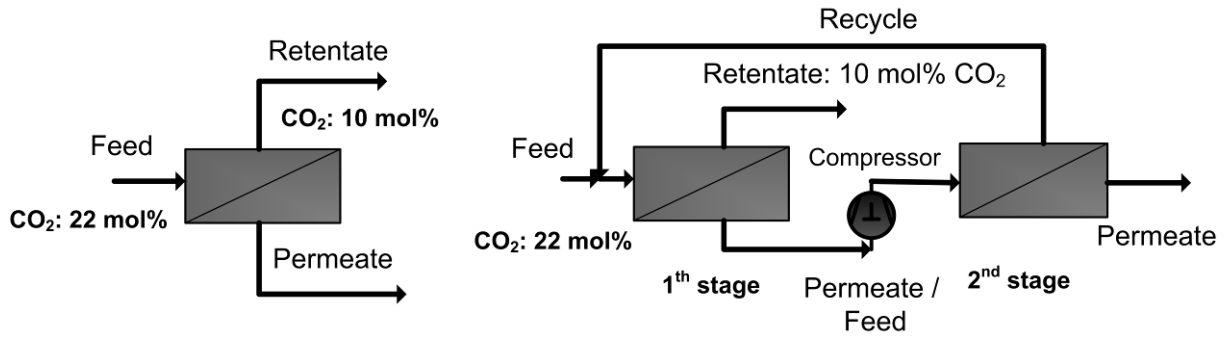


Figure 7. Left side: One stage membrane process – right side: Two stage membrane process

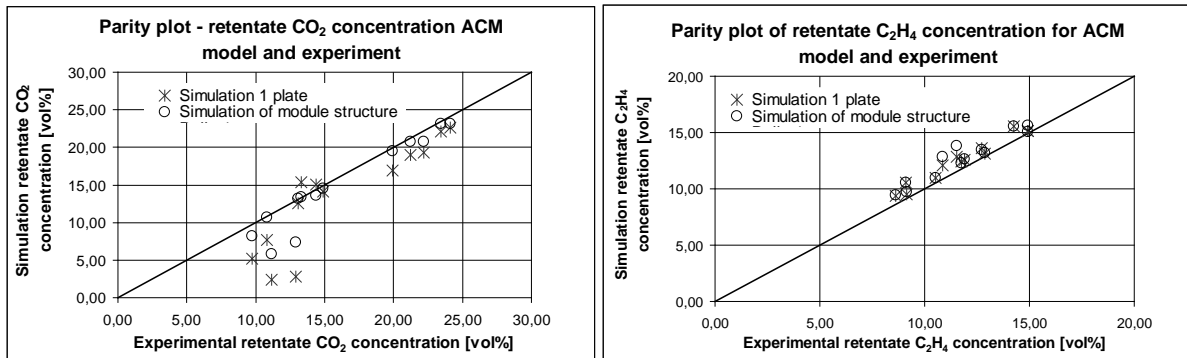


Figure 8. Parity plot between experimental and simulation retentate results for CO<sub>2</sub> concentration (left side) and C<sub>2</sub>H<sub>4</sub> concentration (right side)

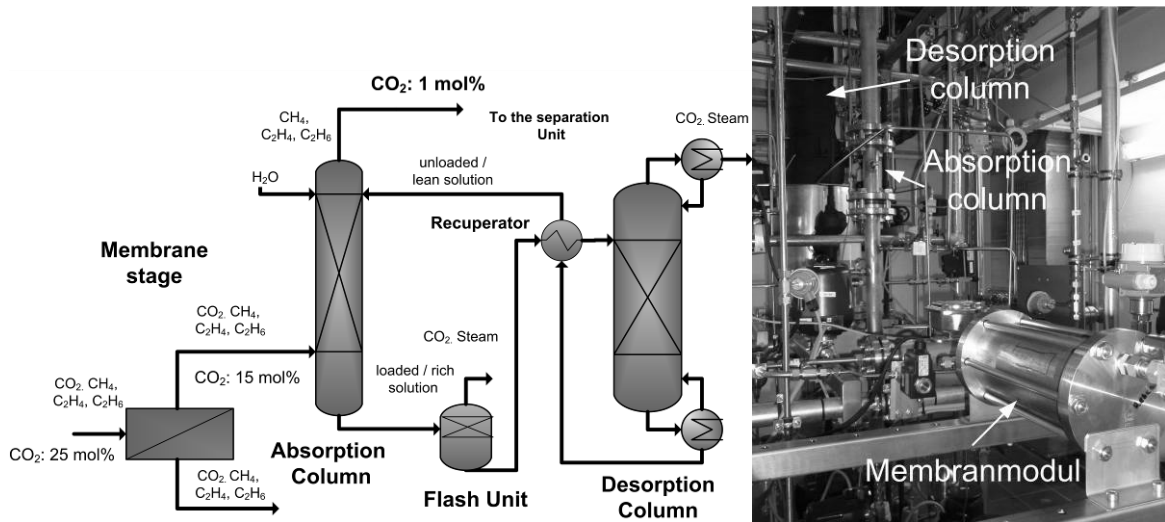


Figure 9. Left side: Flow diagram of the hybrid CO<sub>2</sub> capture process: combined membrane and absorption process; right side: mini-plant design for experimental investigations

## Tables

**Table 1.** Process condition and design task of the CO<sub>2</sub> capture

Gas temperature	Gas pressure	CO <sub>2</sub>	C <sub>2</sub> H <sub>4</sub>	CO <sub>2</sub> removal
40 °C	32*10 <sup>5</sup> Pa	25 mol%	18 mol%	90%

**Table 2.** Base case design of a conventional CO<sub>2</sub> capture process

System pressure	Solvent flow	Gas load	MEA concentration	Solvent regeneration	Absorption packed height	Thermal Energy demand
32*10 <sup>5</sup> Pa	150 kg/hr	0.7 Pa <sup>0.5</sup>	30 wt%	47 %	5 m	2.79 MJ/kg <sub>CO<sub>2</sub></sub>

**Table 3.** Process design and experimental setup

Absorption operation pressure	Absorption column diameter	Absorption packed height	specific packing surface <sup>1</sup>	Desorption operation pressure	Desorption column diameter	Desorption packed height	specific packing surface <sup>2</sup>
32*10 <sup>5</sup> Pa	0.04 m	5 m	450m <sup>2</sup> /m <sup>3</sup>	2.5*10 <sup>5</sup> Pa	0.1 m	4 m	350m <sup>2</sup> /m <sup>3</sup>

<sup>1</sup>Rombopak 12M for the absorption column <sup>2</sup> Rombopak 9M for the desorption column

**Table 4.** Preliminary experimental study conditions

Absorption pressure	Gas load	Liquid load	CO <sub>2</sub> raw gas concentration	Reboiler duty	Desorption pressure	Solvent flow rate
10*10 <sup>5</sup> Pa	0.45 Pa <sup>0.5</sup>	15-16 m <sup>3</sup> /m <sup>2</sup> h	15 vol%	3.41 kW	1.5/2/2.5*10 <sup>5</sup> Pa	15-20 kg/hr



**Table 5.** Results of desorption top pressure study

Desorption top pressure	CO <sub>2</sub> Pure gas concentration	Captured CO <sub>2</sub>	Specific energy input [MJ/kg <sub>CO2</sub> ]
1.5*10 <sup>5</sup> Pa	1.83 vol%	1.71 kg/hr	7.34
2*10 <sup>5</sup> Pa	1.21 vol%	1.77 kg/hr	7.09
2.5*10 <sup>5</sup> Pa	1.45 vol%	1.73 kg/hr	7.25

**Table 6.** Process condition and design task of the CO<sub>2</sub> capture

Gas temperature	Gas pressure	Gas load	CO <sub>2</sub>	C <sub>2</sub> H <sub>4</sub>	CH <sub>4</sub>	N <sub>2</sub>
40 °C	32*10 <sup>5</sup> Pa	0.33 Pa <sup>0.5</sup>	25 vol%	18 vol%	17 vol%	40 vol%

**Table 7.** Experimental base case results for 90% CO<sub>2</sub> capture from OCM reaction gas stream

Liquid load	Solvent flow	$\alpha_{\text{loaded}}$	$\alpha_{\text{unloaded}}$	Desorption pressure	Reboiler duty	Ethylene loss	Thermal Energy demand
m <sup>3</sup> /m <sup>2</sup> h	kg/hr	mol <sub>CO2</sub> /mol <sub>MEA</sub>	mol <sub>CO2</sub> /mol <sub>MEA</sub>	10 <sup>5</sup> Pa	kW	%	MJ/kg <sub>CO2</sub>
42.3	55	0.45	0.39	2	4.7	6	5

**Table 8:** Substances properties data (Bird, 2007)

Component	State 25°C, 1*10 <sup>5</sup> Pa	Molar mass [g/mol]	Boiling Point 1atm[°C]	Melting Point 1atm[°C]	kinetic Diameter $\sigma$ [Å]	Critical Properties	
						T <sub>c</sub> [K]	p <sub>c</sub> [Pa]
Methane	vapour	16	-162	-182	3,8	191,1	45,8*10 <sup>5</sup>
Ethylene	vapour	28	-103,72	-169,18	4,228	282,4	50*10 <sup>5</sup>
Ethane	vapour	30	-89	-183	4,388	305,4	48,2*10 <sup>5</sup>
Nitrogen	vapour	28	-195	-210	3,667	126,2	33,5*10 <sup>5</sup>
Carbon Dioxide	vapour	44	Over critical gas		3,996	304,2	72,8*10 <sup>5</sup>

**Table 9:** Process alternatives and indicators for separation processes (Barnicki, 1992)

Process alternative	Indicator
Cryogenic Distillation	Relative volatility
Physical Absorption	Separation factor for gas solubility using Henry's approach
Molecular Sieve Adsorption	Difference in shape size and kinetic diameter
Equilibrium limited Adsorption	Ratio of the equilibrium loading for the key components
Membrane Separation	Separation factor, ration of the component permeability
Chemical Absorption	Chemical family of the components
Condensation	Difference in normal boiling point
Catalytically conversion	Product Worth

**Table 10:** Commercial available adsorbents form (Barnicki, 1992)

category	nominal aperture size [Å]	Zeolite Type
5	3	3A Linde 3A Davison
4	4	4A Linde, 4A Davison
3	5	5A Linde, 5A Davison
2	8	10X Linde
1	10	13 X Linde, 13X Davison

**Table 11.** Selectivity for a membrane area of 0.5 m<sup>2</sup>

	CA	PEO	POMS	PI
S <sub>CO<sub>2</sub>/C<sub>2</sub>H<sub>4</sub></sub>	12,24	3,5	1,26	16,5
S <sub>CO<sub>2</sub>/C<sub>2</sub>H<sub>6</sub></sub>	14,25	2,75	1,04	54,55
S <sub>CO<sub>2</sub>/CH<sub>4</sub></sub>	17,6	14,1	3,28	39,94

**Table 12.** Membrane sheet parameter

Length	0.08 m
Wide	0.07 m
Number of sheets	44
Numbers of compartments	7
Structure (sheets in the compartment)	7-7-6-6-6-6-6

**Table 13.** Preliminary experiments for the PI membrane module

Pressure	[Pa]	5*10 <sup>5</sup> , 10*10 <sup>5</sup> and 32*10 <sup>5</sup>
CO <sub>2</sub> concentration	[vol%]	15 and 25
Velocity	[m/s]	0.25 – 0.8

**Table 14.** Design and results of the membrane unit in the hybrid process

Raw gas pressure	Membrane area	Membrane material	CO <sub>2</sub> Feed	CO <sub>2</sub> removal	Ethylene loss
32*10 <sup>5</sup> Pa	0.5m <sup>2</sup>	matrimide	25 vol%	50%	13,75 %

**Table 15.** Design and results of the absorption unit in the hybrid process

Absorption column height	Liquid flow	Absorption Solvent	CO <sub>2</sub> raw gas	CO <sub>2</sub> removal	Ethylene loss
2.5 m	55 kg/hr	30wt% MEA	15 vol%	40%	10,79

**Table 16.** Overall performance of the hybrid process

Thermal energy demand	CO <sub>2</sub> removal	Ethylene loss
2.75 MJ/kg <sub>CO2</sub>	90%	13,3